



# Nonlinearity of compression behavior of 3D-epoxy reinforced with carbon fibers composites

S.V. Slovikov, A.V. Babushkin, M.D. Gusina

*Center of Experimental Mechanics, Perm National Research Polytechnic University, Russia*

*sslovikov@ya.ru, <https://orcid.org/0000-0003-3884-3882>*

*bav651@ya.ru <https://orcid.org/0000-0001-8411-757X>*

*kersnyvlk@gmail.com <https://orcid.org/0009-0007-3648-3867>*

**ABSTRACT.** Modern technological make it possible to produce three-dimensional (3D) reinforcement for polymer composite materials. The tasks of experimental research and analysis of the deformation process of new composite materials for aviation purposes taking into account the nonlinearity of mechanical behavior become actual.

The paper presents an experimental study of the mechanical compression behavior of composite material specimens made of 3D woven carbon fiber preforms using the pressure impregnation technology (Resin Transfer Molding method with a pairwise interlayer reinforcement and a longitudinal layer). Compression mechanical tests were carried out on specimens using a universal system of electromechanical testing Instron 5882 and a system of 3D analysis of displacement and strain fields on the surface. Tests were conducted in accordance with ASTM D 3410 recommendations and using specialized tooling. Consideration of nonlinearity parameter during experimental data processing is proposed. The importance of determining the values of critical deformation in compression as a parameter characterizing the moment of the beginning of fracture is noted. The comparison of strength, elastic and deformation properties of carbon-fiber composite materials made using the same technology from fibers and binders from different manufacturers is carried out. The experimental diagrams "stress-strain" and their approximating dependences taking into account the nonlinearity function  $\omega$  are obtained. The type of functions  $\omega$  of the studied materials is defined, the linear approximation of dependence of functions  $\omega$  on strain is substantiated. Values of strength limits, elastic modulus, nonlinearity coefficient and critical damage were obtained, statistical processing of the obtained results and their analysis were carried out.

**KEYWORDS.** Carbon-fiber composite, Polymer binder, Spatially reinforced composite, Nonlinearity, Mechanical behavior, Compression, Strength, Digital image correlation.



**Citation:** Slovikov, S.V., Babushkin A.V., Gusina. M.D., Nonlinearity of compression behavior of 3D-epoxy reinforced with carbon fibers composites, *Frattura ed Integrità Strutturale*, 66 (2023) 311-321.

**Received:** 08.08.2023

**Accepted:** 19.09.2023

**Online first:** 20.09.2023

**Published:** 01.10.2023

**Copyright:** © 2023 This is an open access article under the terms of the CC-BY 4.0, which permits unrestricted use, distribution, and reproduction in any medium, provided the original author and source are credited.

## INTRODUCTION

Recently, the innovative development of advanced industries is often associated with the substitutive application of composite materials (CM). In particular, the current development trends in the field of production and application of reinforced plastics based on high-strength fibers for aviation industry are given in works [1-3]. In [4] the feasibility and experience of using perspective polymer composites in constructions of nodes and parts of aviation power plants and rocket and space equipment are considered. The works [5, 6] are devoted to consideration of innovative development of advanced technologies to be implemented in automated processes of manufacturing three-dimensional reinforced aerospace composite structures.

Modern technological capabilities make it possible to produce three-dimensional space-reinforcing fillers for polymer composites. 3D structures made of composite materials are used in various industries in the production of critical parts and structural elements. In this case their considerable strength in transversal direction is realized, which, in contrast to layered structures, provides conservation of fibrous plastics in the process of their operation. The works [7, 8] consider the application of various volumetrically reinforced polymer composites in technical applications.

Because of the widespread use of composite materials in the production of industrial products, there is a need for various studies of their mechanical behavior. So, in [9] the methods of tests of composite materials under nontrivial loading conditions are considered and analyzed. The problems of determining the mechanical characteristics of composite materials in conditions of fatigue and complex stress-strain state, under the action of static loads and different temperatures are solved. Experimental studies of the effect of operating conditions on the mechanical properties for different classes of polymer composites are described in [10-13]. Later, the obtained data are used in structural calculations in the systems for mathematical modeling of the operating conditions of the materials used [14, 15]. At the same time, the design of structures requires both the characteristics of the rigid elastic material and the strength to adequately estimate the technically permissible strength ranges and calculate the strength criteria.

A complete and adequate analysis and description of the strain diagram requires the use of the concept of strain damageability of the material, at least to the limit of time resistance, and possibly even more. Damage to materials occurs both during production and during use of the product. The size and location of the defects affect the mechanical properties of CMs [16-19]. A common method of quantitative description of the damage process is the use of the damage coefficient [20, 21]. In modern models, considerable attention is also paid to the phenomena of damage accumulation during material deformation [22, 23].

The purpose of this work is an experimental study, analysis and formation of a database on nonlinear deformation of new composite materials. The novelty of the work is associated with the development and improvement of methods for experimental studies of deformation patterns, obtaining new experimental data on mechanical behavior and describing the nonlinearity of the behavior of structural CMs before the beginning of destruction.

## RESEARCH MATERIALS

In this study, mechanical compression tests were carried out on polymer CMs with woven carbon fiber filaments in an epoxy binder matrix. The samples were made of materials made of Umatex UMT49 carbon filament (Dipchel LLC, Russia), VSE-59 binder (FSUE VIAM), Torayca T800H carbon filament and Toray TC350 binder (Toray Composite Materials America, Inc.).

The Properties of epoxy resin and carbon fibers are presented in the Tab. 1.

Samples of 3D carbon plastics in 4 combinations (types) of reinforcing knitted preforms and binders were investigated: T800-T350, T800-VSE59, UMT49-T350 and UMT49-VSE59. Samples were cut from the plates in two directions (along the base of the 3D fabric and along the weft) in 5(6) samples of each type. The material slabs are made according to the schemes of weaving 3D woven preforms with impregnation by Resin Transfer Molding (RTM) [24] with layer-to-layer interlacing and transversal sealing (Layer to layer interlocked with warp). The overall process of board molding consists of several stages, the first of which is the stage of forming the preform - a reinforcing fiber system of a given structure. Next, the "dry" preform is placed in special equipment (rigid die and punch with hermetic connection) for impregnation (RTM itself) and final molding. The impregnation process is carried out by a vacuum compressor through a system of nozzles, and is monitored by binder sensors. At the end of the impregnation process, the binder supply is stopped, the punch compresses the workpiece with a predetermined pressure to ensure a predetermined ratio of component volume fractions, and excess binder is expelled through binder sensors.



Material	Elastic modulus, GPa	Tensile strength, MPa	Strain at Failure, %	Density, g/cm <sup>3</sup>	Cure, °C	Dry T <sub>g</sub> (by DMA), °C	Wet T <sub>g</sub> (by DMA), °C
T800	294	5490	1.9	1.81	-	-	-
UMT49	260	4900	1.8	1.78	-	-	-
T350	-	-	-	1.30	177	191	160
VSE59	-	-	-	1.24	176	188	159

Table 1: Materials properties.

## METHODOLOGY

During quasi-static compression of bulk-reinforced CMs, initially the matrix cracks and then the fibers fail. The primary defects occur in the areas of the lowest values of the fracture strain limit. For metallic materials, this is usually referred to as the "elastoplastic deformation region" or "plasticity with hardening" on the strain diagram; for CMs in compression, this is the area of accumulation of dispersed damage.

The peculiarity of the mechanical behavior of CM requires that the nonlinearity of the mechanical behavior of the material, as a function equivalent to the reduction of the effective cross section of the sample, be taken into account [20, 21]. Then, the dependence of stresses ( $\sigma$ ) on strains ( $\varepsilon$ ) can be represented by the formula:

$$\sigma(\varepsilon) = E(1 - \omega(\varepsilon)) \quad (1)$$

where  $\omega$  is a function characterizing the nonlinearity of the mechanical behavior before the beginning of failure,  $E$  – elastic modulus.

If we assume that the dependence of the function  $\omega$  on the strain is linear, then the dependence is valid:

$$\omega(\varepsilon) = k\varepsilon \quad (2)$$

where  $k$  is the nonlinearity coefficient.

The adequacy of this hypothesis for the studied materials will be shown below.

Then formula (1) is a polynomial of the second degree:

$$\sigma(\varepsilon) = E\varepsilon - Ek\varepsilon^2 \quad (3)$$

The experimental data can be approximated by the method of least squares by formula (3).

In compression tests it is difficult for the experimenter to accurately determine the strains on the material specimen. Finding an extensometer in the loading area is either technically impossible (extensometer dimensions are larger than the working area of the specimen), or the specimen is damaged when it fails. Using an extensometer according to the standard recommendation for such materials leads to unacceptable errors [25]. Estimation of strain by the external elements of the loading system also leads to large errors that often do not allow estimating the damage parameter in the experiment. At present, three-dimensional digital optical systems based on the method of digital image correlation are widely used in scientific research [26-28]. One of such systems is the Vic-3D system [29-31], the use of which removes the problem of exact determination of the strain before the specimen fracture under compression.

The compressive strength, defined as the ratio of the maximum load to the cross-sectional area of bulk-reinforced composites, is often not an indicator of the strength of the material under study. Since there is often a situation when the test sample has already received critical damage to the matrix and fibers, and the force is still increasing. Only a sharp change in the strain rate, as well as a violation of the continuity of the field fixed by Vic3D due to a crack, indicates that the material is destroyed.

It should be emphasized that the limit of applicability of the description of the mechanical behavior of structural carbon plastics by the formula (3) is obviously the critical damage (critical strain). Reaching the critical damage (i.e., significant destruction of the matrix) comes before reaching the compressive strength limit, which is defined as the time resistance.

The fact of these irreversible failures is a sharp change of strain in the compression diagram or, more often, the destruction of the strain field, which indicates the occurrence of a significant crack in the material.

When analyzing the stress-strain diagram, such a criterion may be the deviation from the theoretically found function:

$$\varepsilon_{cr} \Rightarrow \dot{\sigma}^*(\varepsilon) < \dot{\sigma}(\varepsilon) + \delta_\varepsilon$$

where  $\dot{\sigma}^*(\varepsilon)$  – is the derivative of the curve approximating the experimental values,  $\delta_\varepsilon$  - is the error of the experimental data, mainly related to the combined error (rattle) of the measuring instruments - force sensor and Vic-3D extensometer. It is also possible to fix a jump change in the strain value by an amount greater than the measurement error:

$$\varepsilon_{cr} \Rightarrow \varepsilon_i^* < \varepsilon_i + \delta_\varepsilon$$

where  $\varepsilon_i^*$  – strain values on the curve approximating the experimental data,  $i$  – time moment of collecting information from sensors of measuring,  $\delta_\varepsilon$  – measurement error equal to the error of the extensometer Vic-3D.

If the critical damage  $\omega_{cr}$  represents the limit value of the nonlinear function, after which the failure progresses avalanche-like, cracks form on the surface and the deformation of the sample by the Vic-3D system cannot be fixed (the continuity of the deformation field of the Vic-3D system is broken), then since  $\omega$  is proportional to strain:

$$\omega_{cr} = k\varepsilon_{cr}.$$

## EXPERIMENT

The tests were performed on an Instron 5882 electromechanical system in accordance with ASTM D 3410 recommendations [32]. Standard shaped specimens and recommended tooling were used for the tests (Fig. 1).

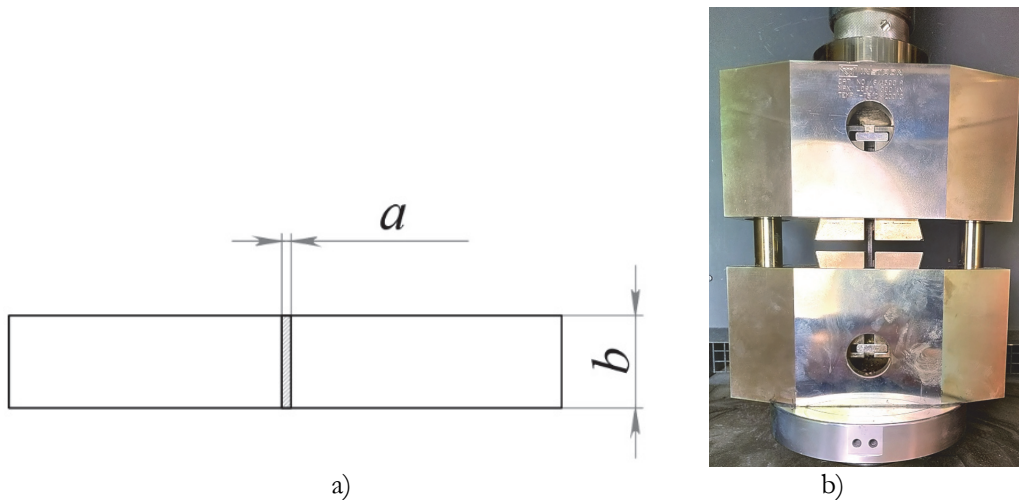


Figure 1: Sketch of sample (a) and photo of tooling (b) according to ASTM D3410:  $a = 4.5 \pm 0.2 \text{ mm}$ ,  $b = 25.1 \pm 0.3 \text{ mm}$ .

Sample thickness "a" and sample width "b" were measured using a Mitutoyo digital micrometer head, the error of the device is  $\pm 0.004 \text{ mm}$ . The traverse travel speed is  $1.5 \text{ mm/min}$ . The accuracy of load measurement is  $0.5\%$  of the measured value. The strain was determined using a three-dimensional digital optical system Vic-3D (Fig. 2) equipped with two cameras with a resolution of 4 megapixels.

The strain was recorded using an additional software module of the "virtual extensometer" video system. Its principle of operation is similar to the contact extensometer and consists in tracing the mutual displacement between two points on the surface of the samples according to the applied force. The appearance of tooling with the compression test fixture installed is shown in Fig. 2 in accordance with ASTM D 3410.

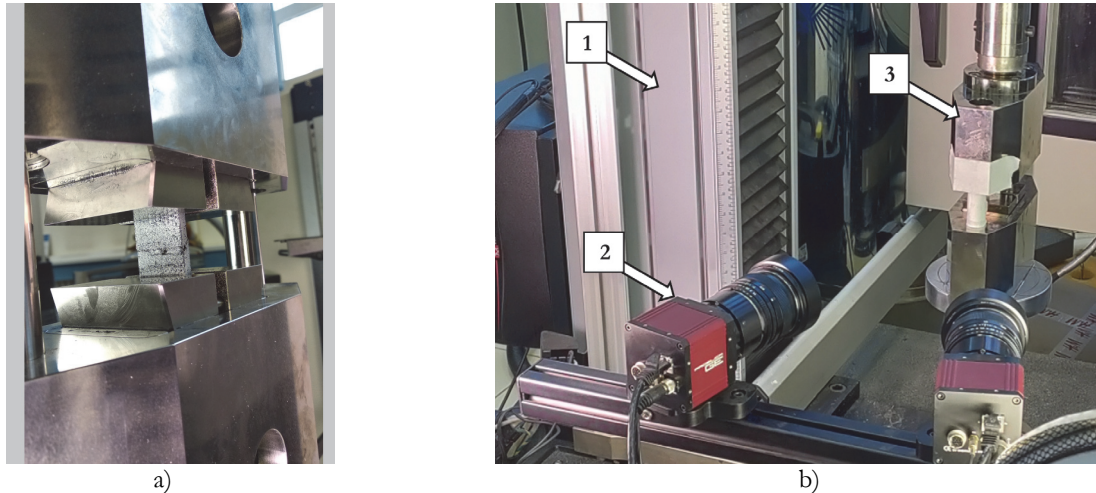


Figure 2: Image of the specimen in the Instron 5882 tooling (a) and Vic 3D system setup (b: 1- Instron 5882, 2- Vic 3D, 3- tooling ASTM D 3410) for compression tests.

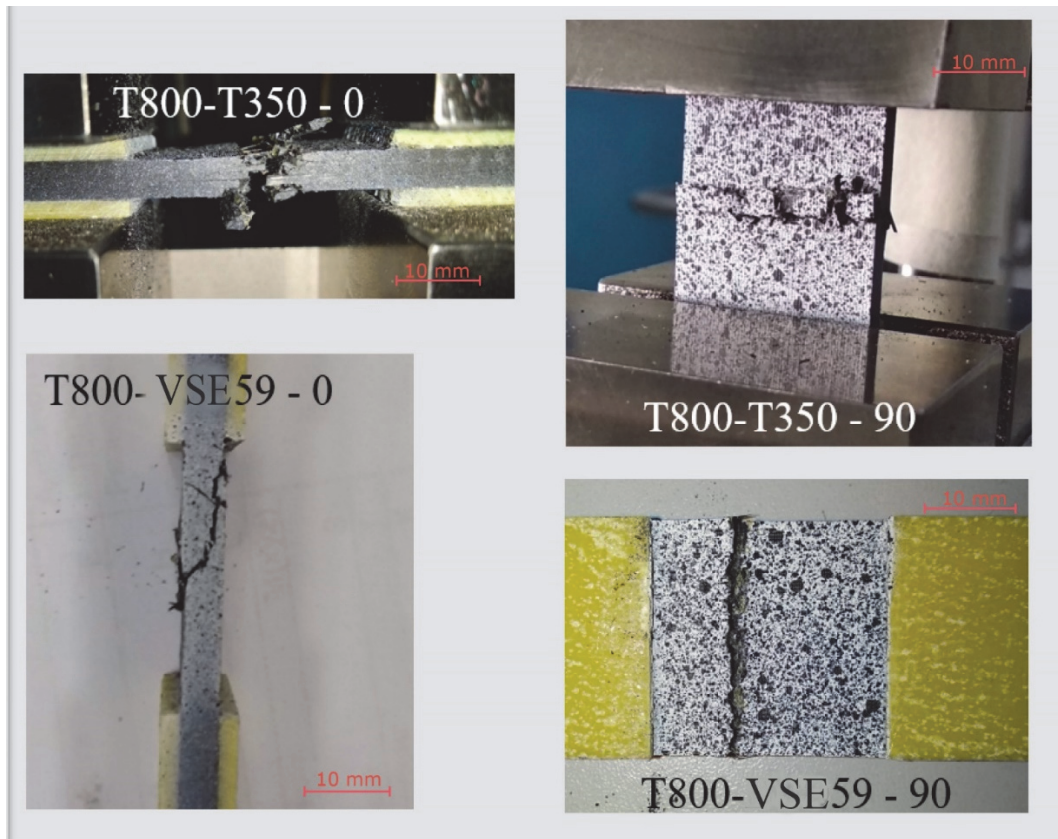


Figure 3: Fracture examples of T800H samples.

Tests are performed in accordance with ASTM D 3410. And as a result of the test the following characteristics are determined: maximum load in compression (kN), ultimate compressive strength (MPa), modulus in compression (GPa), fracture classification according to ASTM. According to the test results for each group of specimens the diagrams "stress - strain" are plotted, the mathematical expectations of the required values are determined with a confidence interval for the 95% probability.

Marking of the samples is done as follows:

- "T800-T350" is a combination of Torayca - T800H carbon filament and Toray TC350 binder in a sample,
- «UMT49-BCЭ59» – UMT49 carbon filament and VSE-59 binder are used,

- T800-VE59 - Torayca - T800H carbon filament and "VSE-59" binder,
- "UMT49-T350" - carbon filament UMT49 and binder brand TC350,
- "0" indicates that the sample is cut along the warp, "90" along the weft.

Examples of sample fractures are shown in Figs. 3 & 4 and in general they have a similar character. There is no such type of fracture as delamination, which, for example, is typical in compression according to ASTM D 3410 of the same samples, but made by the more common prepreg technology.

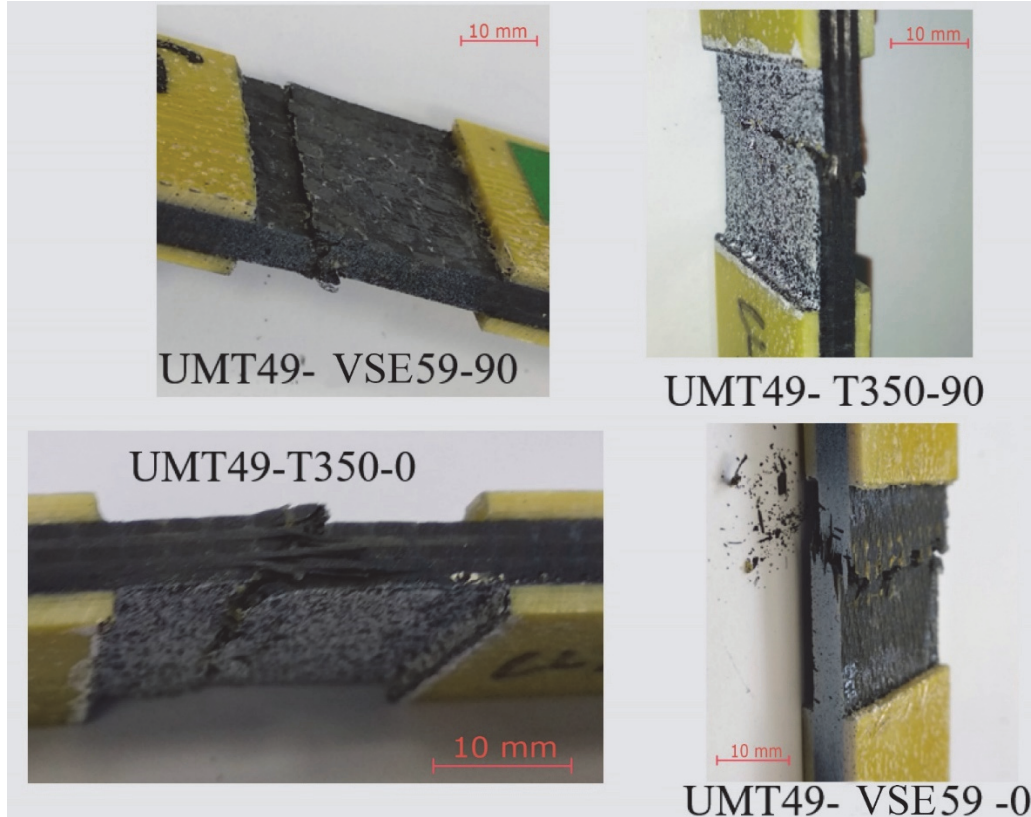


Figure 4: Fracture examples of UMT49 samples.

Evaluating the production technology of these samples, it is worth noting its high stability, as all samples had a very small variation of "load-displacement" diagrams, which could be caused by the presence of manufacturing defects, such as voids that occurred during pressure impregnation.

## RESULTS AND DISCUSSION

The results of the conducted studies in the form of stress – strain dependencies are presented in Fig. 5 and Fig. 6 for eight types of samples. For each sample, an approximating curve for function (3) is constructed using the least squares method, taking into account the nonlinearity. The mathematical expectation of the parameters of this function (the elastic modulus  $E$  and the nonlinearity coefficient  $k$ ) for each of the eight types of samples is determined and an approximating curve is constructed based on them (indicated by a black dotted line in Figs. 5 & 6) on each set of diagrams. For the samples of materials used in this study, not taking into account the nonlinear behavior leads to the fact that under loads, for example, 80% of the destructive load, the strain error is more than 14% of the current value.

Approximation of the stress-strain relation of each test specimen by Eqn. (3) gives a sufficiently accurate description (not less than 0.996 coefficient of approximation reliability) of mechanical behavior on the stress-strain diagram. However, in spite of the complete certainty of the values required for the integral approximation of the experimental strain curves by the polynomial (3), the identification and analysis of the functions  $\omega$  themselves, characteristic for this class of composite materials, appears to be an independent and very important task. It is also necessary to substantiate a linear approximation of these functions.

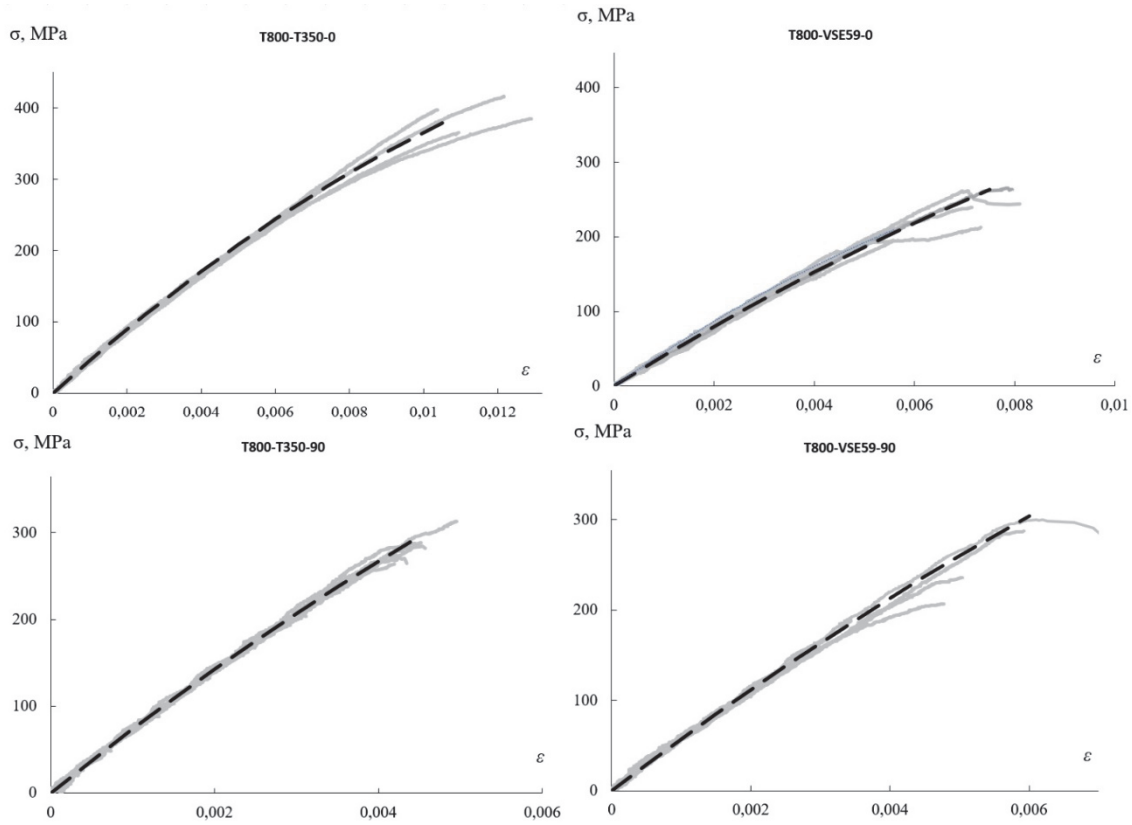


Figure 5: Stress-strain diagrams for samples T800H (solid line - test data dotted line - approximation of test data).

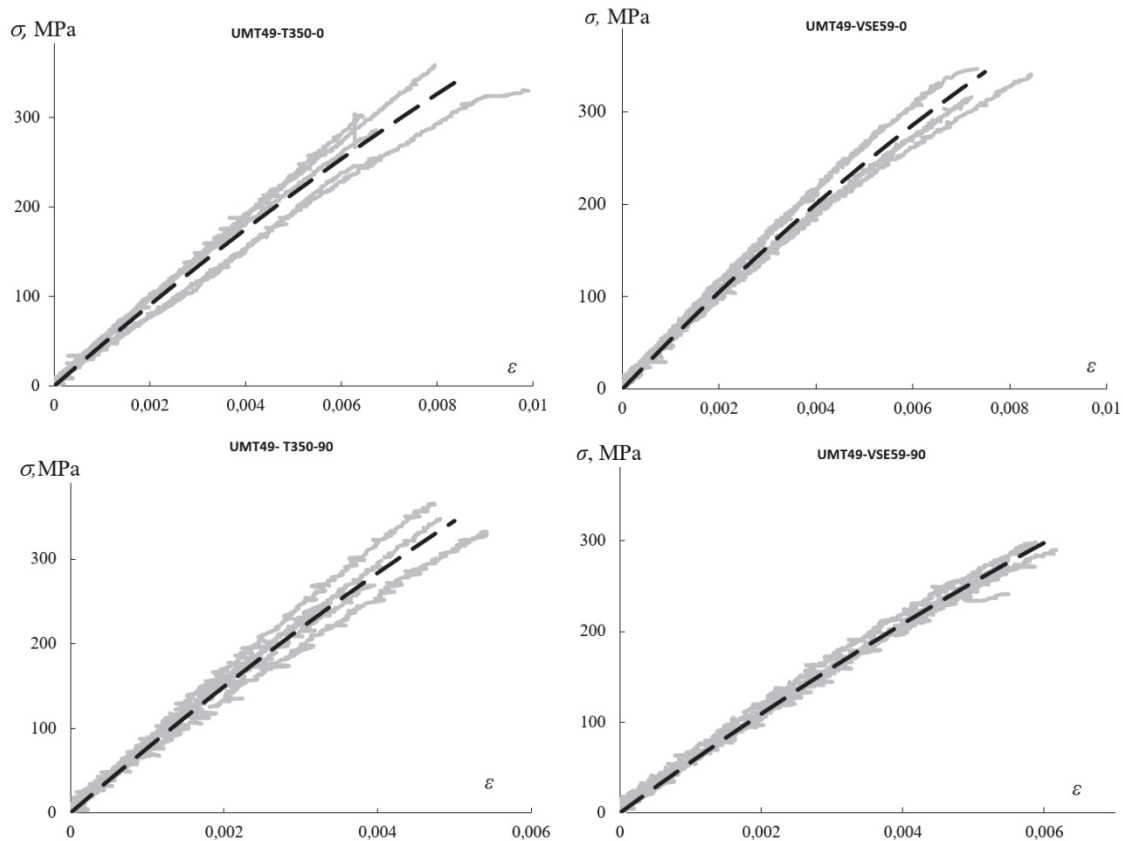


Figure 6: Stress-strain diagrams for UMT49 samples (solid line - test data dotted line - approximation of test data).

The construction of experimental functions  $\omega$  is based on the processing and analysis of strain diagrams, which are an array of pairwise values (coordinates of points) of conditional stresses and strains obtained using the built-in force sensor and the ViC-3D system, respectively.

The type and nature of the function  $\omega$  will be determined by recalculating the coordinates of the points of the strain diagram according to the formula (1). In this case, the left boundary of the range of the function's existence will be determined by the inequality:

$$\omega(\varepsilon) = 1 - \left( \frac{\sigma}{E\varepsilon} \right) > 0$$

where  $\sigma$  and  $\varepsilon$  are coordinates of the points in the strain diagram. The right boundary is defined by the critical value of this function defined above.

Examples of functions  $\omega$  of the materials under study and their linear approximations are shown in Fig. 7. The analysis of  $\omega$  functions is complicated by small strain values of the sample material and the size of the strain field recorded by the video system (25x17 mm), which is comparable to the error of strain of movements of the digital optical system of  $\pm 2$  mcm, since it leads to "sawtooth" curves in the diagrams. However, the analysis and practice of experimental work show that the fluctuations are primarily associated with the reaction of the recording equipment in the area of small values of the measured quantities to the change of structural phases of the CM deformation process. Three phases of deformation and damageability of materials can be distinguished: elastic deformation without macro manifestation of damageability, steady growth of damageability and overcritical, avalanche-like, uncontrolled growth. Thus, the increased amplitude of fluctuations at the initial stage of the function  $\omega$  indicates the reaction (excitation) of the recording equipment to the transition from elastic deformation to the obvious, noticeable growth of the function  $\omega$ . Then the bounce stabilizes, and the nonlinearity function  $\omega$  steadily increases. The general trend of the functions  $\omega$ , free from fluctuations, is most adequately approximated for these materials linearly by formula (2).

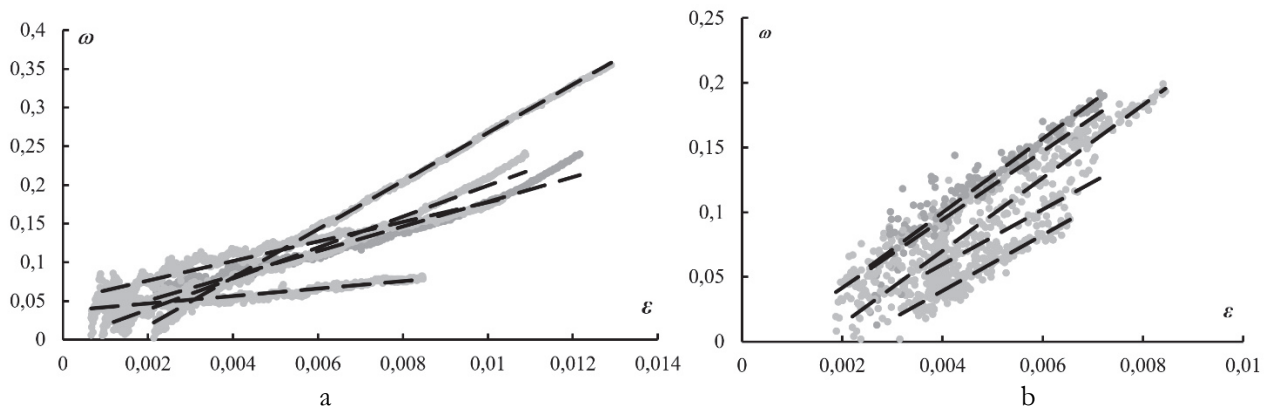


Figure 7: Examples of function  $\omega$  (point) and their linear approximation (dotted line): a) T800-T350-0, b) UMT49-VSE-59-0.

The mechanical characteristics determined during the study are presented as histograms in Fig. 8. Estimates of the values were obtained by Student's method, where the confidence intervals were determined with a 95% probability.

As a result of tests carried out on samples manufactured (produced) using the same technology on the same equipment from components similar in their properties, as a result we have a different scatter of test diagrams and we assume that this is influenced by the interaction of fibers and matrices from different manufacturers, which is manifested in stability (small scatter) of stress-strain diagrams.

In general, it should be noted a rather high stability of the technology of material manufacturing. Moreover, the samples were made from different slabs. There is also less stability of production technology from raw materials of LLC "Dipchel" and FSUE "VIAM" - the confidence interval of variation of values is 10% more than for samples from raw materials produced by Toray.



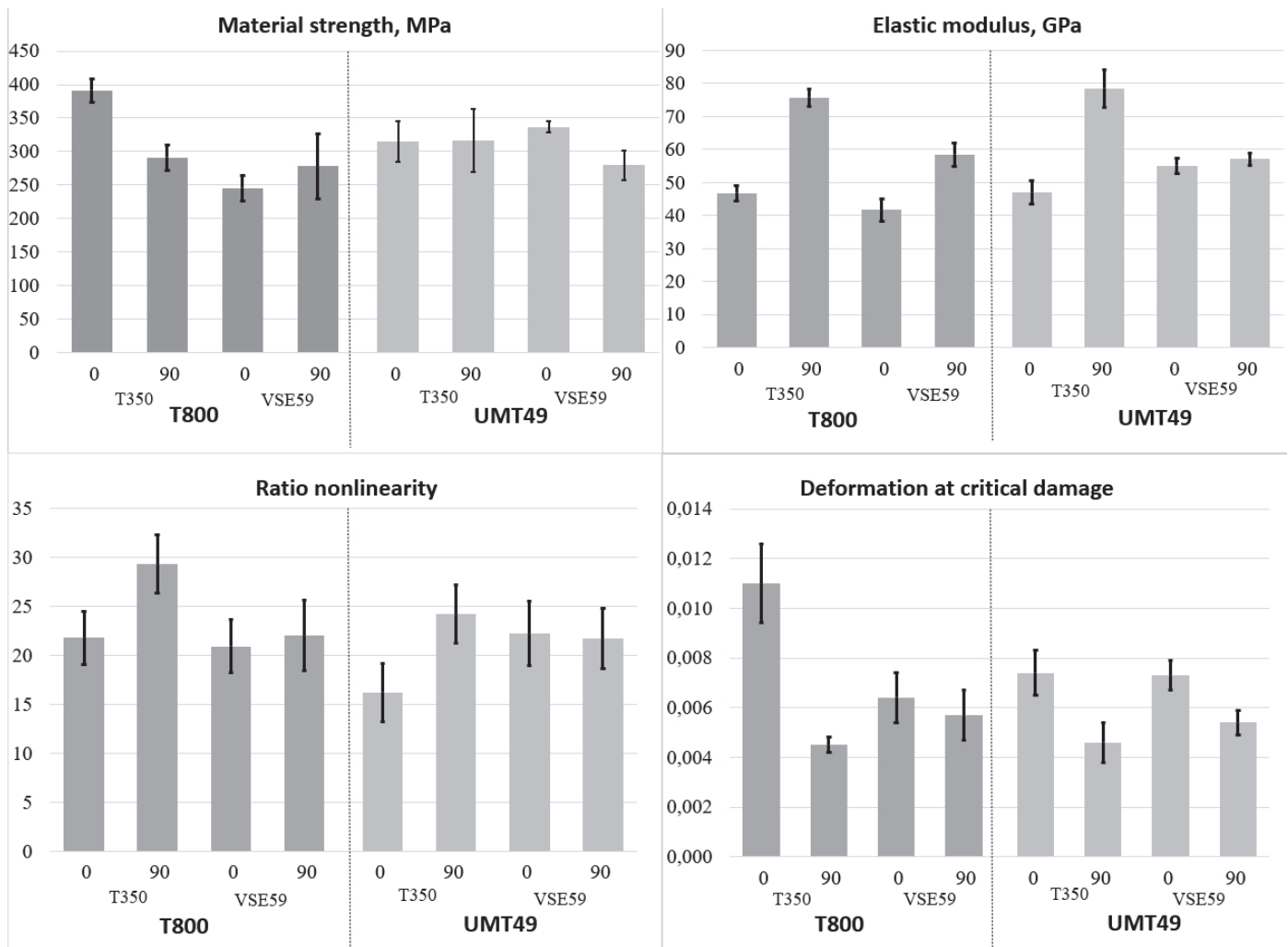


Figure 8: Mechanical parameters of the studied CM samples (0,90 - reinforcement directions).

## CONCLUSIONS

In the course of the study, the ultimate strength, modulus of elasticity and the maximum value of strain of the material for 4 types of composite materials were determined.

Evaluating the production technology of the investigated composite materials, we can conclude that the mechanical behavior of the samples made from the raw materials of Toray production is more stable (which was estimated by the value of confidence intervals of variation) and it is 10% higher than that of the samples from the raw materials of LLC "Dipchel" and FSUE "VIAM".

To analyze of mechanical behavior during compression of a CM, it is proposed to use a function  $\omega$  describing the nonlinear dependence of stress on strain up to the critical value  $\omega_c$ . The function  $\omega$ , it is proposed to approximate linearly.

In evaluating the material, it is proposed to determine the nonlinear mechanical behavior and the value of the critical strain in compression.

## ACKNOWLEDGEMENTS

This work was carried out with the support of the Russian Science Foundation (Project No 21-79-10205, <https://rscf.ru/project/21-79-10205/>, accessed on 13 December 2022) at the Perm National Research Polytechnic University.



## REFERENCES

- [1] Kablov, E.N. (2012). Strategic directions for the development of materials and their processing technology for the period up to 2030. *Aviation Materials and Technologies*, 5, pp. 7-172.
- [2] Subbotin, V.V., Grinev, M.A. (2013). Experience in the use of materials manufactured by FSUE "VIAM" and PORCHER in the construction of components and parts of aircraft power plants made of polymer composite materials. *Material science and technology news*, 5.
- [3] Anoshkin, A.N., Zuiko, V.Y., Shipunov, G.S., Tretyakov, A.A. (2014). Technologies and problems of composite materials mechanics for production of outlet guide vane for aircraft jet engine. *PNRPU Mechanics Bulletin*, 4, pp. 5-44. doi: 10.15593/perm.mech/2014.4.01.
- [4] Gunyaeva, A.G., Sidorina, A.I., Kurnosov, A.O., Klimenko, O.N. (2018). Polymeric composite materials of new generation on the basis of binder VSE-1212 and the filling agents alternative to ones of Porcher ind. and Toho Tenax. *Aviation Materials and Technologies*, 3(52), pp. 18-26. DOI:10.185 77/2071 -9140-2018-0-3-18-26.
- [5] Dell'Anno, G., Partridge, I., Cartié, D., Hamlyn, A., Chehura, E., James, S., Tatam, R. (2012). Automated manufacture of 3D reinforced aerospace composite structures, *International Journal of Structural Integrity*, 3(1), pp. 22–40. DOI: 10.1108/17579861211209975.
- [6] Ketov, Iu.A. Slovikov, S.V. (2019). Syntactic poly meric composite materials highly completed with granulated foam glass. *Computational Nanotechnology*, 6 (3), pp.39-46. doi:10.33693/2313-223X-2019-6-3-39-46.
- [7] Bilisik, K. (2012). Multiaxis three-dimensional weaving for composites: A review. *Textile Research J.*, 82(7), pp. 725-743. DOI: 10.1177/00405175111435013.
- [8] Evdokimov, A., Donetskii, K., Sidorina, A., Gunyaeva, A. (2019). Manufacture of Three-Dimensional Reinforced Fabric Preforms for Making Aviation Products in Russia and Abroad – a Review, *Fibre Chemistry*, 51(2), pp. 30-33. DOI: 10.1007/s10692-019-10055-y.
- [9] Lobanov, D. S., Babushkin, A. V. (2012). Deformation and fracture of fibrous polymer composites in thermo-mechanical impact conditions. *Proc. of ECCM15: European Conference on Composite Materials*, Venice, Italy, 2428.
- [10] Kucher, N. K., Zarazovskii, M. N., Danil'chuk, E. L. (2013). Deformation and strength of laminated carbon-fiber-reinforced plastics under a static thermomechanical loading. *Mechanics of Composite Materials*, 48(6), pp. 669-680. DOI: 10.1007/s11029-013-9311-0.
- [11] Babushkin, A.V., Lobanov, D., Kozlova, A.V., Morev, I.D. (2013). Research of the effectiveness of mechanical testing methods with analysis of features of destructions and temperature effects, *Frattura Ed Integrità Strutturale*, 24, pp. 89–95. DOI: 10.3221/IGF-ESIS.24.09.
- [12] Nikolaev, E.V., Koren'kova, T.G., Shvedkova, A.K., Valevin, E.O. (2015). Research of an influence of temperature factors on aging of new polymer composite materials for aviation engine nacelle. *TRUDY VIAM*, 3, pp. 1-13. DOI: 10.18577/2307-6046-2015-0-3-12-12
- [13] Lobanov, D., Vildeman, V., Babin, D., Grinev, M. (2015). Experimental Research Into the Effect Of External Actions and Polluting Environments on the Serviceability of Fiber-Reinforced Polymer Composite Materials, *Mechanics of Composite Materials*, 51, pp. 69–76. DOI: 10.1007/s11029-015-9477-8.
- [14] Yankin, A.S., Bulbovich, R.V., Slovikov, S.V. (2017). Mathematical model and experimental studies of behavior of viscoelastic filled polymers under two-frequency loadings, *PNRPU Mechanics Bulletin*, (2), pp. 208–225.
- [15] Slovikov, S.V., Lobanov, D.S. (2020). Mechanical Properties of a Basalt-Fiber-Reinforced Plastic Rod Used in Composite High-Voltage Wires in Torsion and Three-Point Bending, *Mech Compos Mater*, 56(3), pp. 353–360. DOI: 10.1007/s11029-020-09886-2.
- [16] Cantwell, W.J., Morton, J. (1992). The significance of damage and defects and their detection in composite materials: A review, *The Journal of Strain Analysis for Engineering Design*, 27(1), pp. 29–42. DOI: 10.1243/03093247V27I029.
- [17] Armstrong, K., Cole, W., Bevan, G. (2005). Care and repair of advanced composites, *SAE*, pp. 1-28. DOI: 10.4271/R-336.
- [18] Senthil, K., Arockiarajan, A., Palaninathan, R., Santhosh, B., Usha, K.M. (2013). Defects in composite structures: Its effects and prediction methods – A comprehensive review, *Composite Structures*, 106, pp. 139–149. DOI: 10.1016/j.compstruct.2013.06.008.
- [19] Xie, N., Smith, R.A., Mukhopadhyay, S., Hallett, S.R. (2018). A numerical study on the influence of composite wrinkle defect geometry on compressive strength, *Materials & Design*, 140, pp. 7–20. DOI: 10.1016/j.matdes.2017.11.034.
- [20] Kachanov, L. M. (1958). Time of the Rupture Process under Creep Conditions. *Izvestiia Akademii Nauk SSSR, Otdelenie Teckhnicheskikh Nauk*, 8, 26-31 (in Russian).



- [21] Rabotnov, Y. N. (1991). Problems of deformable solid mechanics: selected papers, Science.
- [22] Shliannikov, V.N., Tumanov, A.V. (2018). Force and deformation models of damage and fracture during creep, *Physical Mesomechanics*, 21(3), pp.70-85. doi: 10.24411/1683-805X-2018-13008.
- [23] Turkova, V.A., Stepanova, L.V. (2018). Evaluation of damage accumulation zone in the vicinity of the crack tip: FEM analysis via UMAT procedure, *J. Phys.: Conf. Ser.*, 1096(1), p. 012157. DOI: 10.1088/1742-6596/1096/1/012157.
- [24] Fanguero, R., & Gonigho-Pereira, C. (2011). Fibrous materials reinforced composite for internal reinforcement of concrete structures. In *Fibrous and Composite Materials for Civil Engineering Applications*. Elsevier Ltd. DOI: 10.1016/B978-1-84569-558-3.50008-9
- [25] Strungar, E.M., Yankin, A.S., Zubova, E.M., Babushkin, A.V., Dushko, A.N. (2019). Experimental study of shear properties of 3D woven composite using digital image correlation and acoustic emission, *Acta Mechanica Sinica*, 36, pp. 448–459. DOI: 10.1007/s10409-019-00921-7.
- [26] Wang, Y., Cuitiño, A.M. (2002). Full-field measurements of heterogeneous deformation patterns on polymeric foams using digital image correlation, *International Journal of Solids and Structures*, 39(13), pp. 3777–3796. DOI: 10.1016/S0020-7683(02)00176-2.
- [27] Sutton, M.A., Orteu, J.-J., Schreier, H. (2009). *Image Correlation for Shape, Motion and Deformation Measurements*, Boston, MA, Springer US, DOI: 10.1007/978-0-387-78747-3.
- [28] Strungar, E., Lobanov, D., Wildemann, V. (2021). Evaluation of the Sensitivity of Various Reinforcement Patterns for Structural Carbon Fibers to Open Holes during Tensile Tests, *Polymers*, 13(24), p. 4287. DOI: 10.3390/polym13244287.
- [29] Vil'deman, V.E., Babushkin, A.V., Tretyakov, M.P., Ilyinykh, A.V., Tretyakova, T.V., Ipatova, A.V., Silovikov, S.V., Lobanov D.S. (2011). *Mechanics of Materials. Methods and tools for experimental research*. Publishing House PNRPU.
- [30] Wildeman, V.E., Tretyakov, M.P., Tretyakova, T.V., Bulbovich, R.V., Slovikov, S.V., Babushkin, A.V., Ilyinykh, A.V., Lobanov, D.S., Ipatova A.V. (2012). *Experimental researches of materials the properties under complex thermomechanical effects*, Fizmatlit Publisher
- [31] Tretyakova, T.V., Dushko, A.N., Strungar, E.M., Zubova, E.M., Lobanov, D.S. (2019). Comprehensive analysis of mechanical behavior and fracture processes of specimens of three-dimensional reinforced carbon fiber in tensile tests, *PNRPU Mechanics Bulletin*, (1), pp. 173–183. DOI: 10.15593/perm.mech/2019.1.15.
- [32] ASTM D3410. Standard Test Method for Compressive Properties of Polymer Matrix Composite Materials with Unsupported Gage Section by Shear Loading. (2021).